

See discussions, stats, and author profiles for this publication at: <https://www.researchgate.net/publication/221684147>

Temporal and Spatial Profiling of Internode Elongation-Associated Protein Expression in Rapidly Growing Culms of Bamboo

ARTICLE in JOURNAL OF PROTEOME RESEARCH · MARCH 2012

Impact Factor: 4.25 · DOI: 10.1021/pr2011878 · Source: PubMed

CITATIONS

8

READS

122

5 AUTHORS, INCLUDING:



Kai Cui

Chinese Academy of Forestry

9 PUBLICATIONS 29 CITATIONS

[SEE PROFILE](#)



Cai-yun He

Chinese Academy of Forestry

16 PUBLICATIONS 84 CITATIONS

[SEE PROFILE](#)



Yan-Fei Zeng

Chinese Academy of Forestry

10 PUBLICATIONS 122 CITATIONS

[SEE PROFILE](#)

Temporal and Spatial Profiling of Internode Elongation-Associated Protein Expression in Rapidly Growing Culms of Bamboo

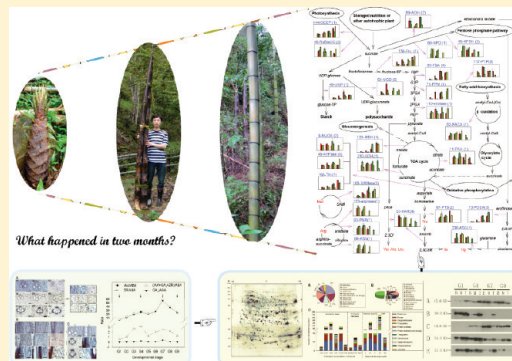
Kai Cui,^{†,‡,||} Cai-yun He,^{†,||} Jian-guo Zhang,^{*,†} Ai-guo Duan,[†] and Yan-fei Zeng[†]

[†]State Key Laboratory of Tree Genetics and Breeding, Research Institute of Forestry, Chinese Academy of Forestry, Beijing 100091, People's Republic of China

[‡]Research Institute of Resources Insects, Chinese Academy of Forestry, Kunming, 650224, People's Republic of China

Supporting Information

ABSTRACT: In natural conditions, culms of developing Moso bamboo, *Phyllostachys heterocycla* var. *pubescens*, reach their final height of more than ten meters within a short period of two to four months. To study this phenomenon, bamboo culm material collected from different developmental stages and internodes was analyzed. Histological observations indicated that the development of culm was dominated by cell division in the initial stages and by cell elongation in the middle and late stages. Development, maturation, and aging in different regions of the culm were studied systematically from the basal to the top internode. The four major endogenous hormones, indole acetic acid, gibberellic acid, zeatin riboside, and abscisic acid appeared to strongly influence the cell elongation phase. A total of 258 spots were differentially expressed in culm development. Of these, 213 spots were identified by MALDI-TOF/TOF MS and were involved in many physiological and metabolic processes including carbohydrate metabolism, cell division, cell expansion, protein synthesis, amino acid metabolism and redox homeostasis. These proteins with different expression patterns constructed an ingenious network to regulate the culm development. Developmental stage-specific and internode-specific protein expression patterns were identified. Protein abundance was regulated temporally and to some extent spatially, and the sequential development from base to apex of bamboo culm was implemented by temporal and spatial expression of enzymes. Results indicate that during development energy was mainly derived from sucrose degradation, as photosynthetic capacity was poor. The regulation of anaerobic and aerobic modes of respiration appeared to play an important role in energy generation. This is the first report on proteomic profiling in bamboo and helps in understanding the regulatory processes in developing culms.



KEYWORDS: *Phyllostachys heterocycla*, internode elongation, histological observations, endogenous hormones, differentially expressed proteins, anaerobic respiration, aerobic respiration, substance and energy metabolism

INTRODUCTION

Nowadays, greenhouse gas emissions and energy shortage have become a bottleneck in the economic development of countries around the world, while exploiting fast-growing and high yielding wood resources is an effective way to overcome these issues. Bamboo is one of the fastest-growing plants on Earth. For example, *Phyllostachys heterocycla* (Moso bamboo) can grow up to a height of 119 cm (47 inches) in 24 h and of 24 m (78.5 feet) in 40–50 days, due to the expansion of individual internodes that are already present in the buds.^{1,2}

Moso bamboo is the most important bamboo species in China and the third most important plant species for timber production. The natural habitat of *P. heterocycla* extends approximately 23°30' to 32°20' N and 104°30' to 122° E. There are 7.4 million acres of bamboo forest (over two-thirds of the total planted bamboo area), which is about 2% of the total forest area in China.¹ It is a large woody bamboo with the

highest ecological, economical, and cultural values among all bamboos in Asia and accounts for 5 billion US dollars of annual forest production in China.^{3,4}

To better understand the growth characteristics and physical properties of bamboo, numerous studies have focused on the general mode of growth and anatomical structure of the culms,^{5–7} and sequential elongation of the internodes from the base to the top has been observed.³ Some internode elongation-associated genes such as *EUI1*, *ACO1*, *SNORKEL1* and *SNORKEL2*, *OsGLU1*, *SSD1*, *CENL1* have been identified in other plants of Gramineae.^{8–13} Compared with other plants of Gramineae, limited molecular information is available for the bamboo subfamily, Bambusoideae, which contains more than 1500 species.¹⁴ Despite the sequencing of a set of cDNAs,^{4,14–17} ESTs¹⁸ and generation of a monoclonal antibody bank,¹⁹ the

Received: December 2, 2011

Published: March 8, 2012



Figure 1. Different developmental stages of *P. heterocycla* culm. G1, freshly unearthed culms; G4, culms covered by a layer of culm sheaths; G7, culms after shedding sheath; G9, culms those stop growing in height before leaf expansion. The estimated culm heights are given in the lower left corner of each panel. A schematic of the three developing internodes is shown in the right panel. The positions indicated by red arrow were sampled.

molecular mechanism underlying the rapid internode elongation remains unclear.

Proteomics is a powerful tool to study global changes in protein synthesis patterns in response to environmental stimuli as well as during development. In this study, we used two-dimensional electrophoresis (2-DE) combined with mass spectrometry (MS) to study protein expression during internode elongation throughout the growth season of Moso bamboo. The identity of the proteins and some of the conclusions drawn were further verified based on light microscopy observations or the use of specific antibodies. To our knowledge, such a detailed investigation of proteome of bamboo has not been reported so far.

MATERIALS AND METHODS

Plant Material

Culm samples from natural population of *P. heterocycla* were harvested in the spring of 2009 from Dagang-Mountain National Nature Reserve in Jiangxi province of China ($27^{\circ}30' - 27^{\circ}50' N$, $114^{\circ}30' - 114^{\circ}45' E$). All samples were collected in the same growing season. Nine developmental stages were defined based on the heights above ground of individual plants: 0.05, 0.20, 0.50, 1.00, 2.00, 3.00, 6.00, 8.50 and 12.00 m, labeled as G1, G2, G3, G4, G5, G6, G7, G8 and G9, respectively. Each culm was divided into three portions (basal, middle and top internodes) according to its height by an equal division method. Thus, the first internode in basal internodes, the longest internode in middle internodes, and the uppermost internode in top internodes were collected separately. Triplicate independent samples (three biological replicates) were cut from culm tissue located in the basal part of each collected internode from different stages as mentioned above (Figure 1). A part of each sample was immediately frozen in liquid nitrogen and stored at $-80^{\circ}C$ until analysis, while the remaining was placed in a buffer for microscopic analysis as described below.

Sectioning and Light Microscopy

Culm tissue samples of about 0.5 cm^3 volume were fixed in FAA buffer (50% ethanol, acetic acid and formaldehyde, 18:1:1 (v/v/v)) and exhausted with aspirator pump. Subsequently, the

tissues were dehydrated by passage through increasing concentrations of ethanol and finally embedded in paraffin. Transverse and longitudinal sections of $8 \mu\text{m}$ in thickness were cut from the FAA fixed cubes on a sliding microtome (LEICA DM 2135, Germany). Sections were stained with a solution of 1% safranin and 0.1% Fast Green sequentially. They were observed with a Zeiss Axiophot light microscope (Zeiss, Jena, Germany). Digital images were analyzed using Zeiss Axio Vision 4.6.

ELISA

The extraction and purification of endogenous hormones indole-3-acetic acid (IAA), gibberellic acid (GA_3), abscisic acid (ABA) and cytokinin zeatin riboside (ZR), was performed according to Wang et al.²⁰ ELISA kits used for estimation of the hormone levels were purchased from China Agricultural University (Beijing, China).

Protein Sample Preparation

Frozen culm tissues (2 g, fresh weight) were ground to a fine powder in liquid nitrogen with 10% poly vinyl pyrrolidone polymer (PVPP) and resuspended in ice-cold extraction buffer containing 10% TCA, 0.07% β -mercaptoethanol (β -ME) in acetone. Homogenates were precipitated overnight at $-20^{\circ}C$. After centrifugation at $12000 \times g$, at $4^{\circ}C$, for 30 min, pellets were washed with precooled acetone containing 0.07% β -ME for 1 h at $-20^{\circ}C$. Then, the pellets were washed twice with 100% precooled acetone and dried for 20 min by vacuum freeze-drying. The lyophilized pellets were resuspended in a rehydration buffer containing 8 M urea, 1% (w/v) DTT, and 2% (w/v) CHAPS. For each sample, 100 mg of lyophilized pellets were dissolved in 1 mL rehydration buffer. The solution was centrifuged at $12000 \times g$ ($4^{\circ}C$) for 30 min and the supernatant was collected. Protein concentration was determined by the method of Bradford.²¹

2-DE and Image Analysis

2-DE was performed using IPGphor system (Amersham Biosciences, Uppsala, Sweden) and IPG dry strips (18 cm, pH 3–10, nonlinear gradient) (GE Healthcare, Buckinghamshire, U.K.). For each sample, 450 μg of protein was placed on a strip saturated in rehydration solution (8 M urea, 2% (w/v) CHAPS, 20 mM DTT, and 0.5% Pharmalyte 3–10, and trace bromophenol blue). Focusing was programmed as follows: 12 h

active rehydration followed by IEF with a gradual increase in the voltage (30–8000 V) and then reaching 40 kVh. After IEF, strips were immediately allowed to equilibrate for 12 min in 10 mL of buffer containing 50 mM Tris–HCl (pH 8.8), 6 M urea, 30% (v/v) glycerol and 2% (w/v) SDS, 100 mg DTT with gentle shaking, followed by addition of 225 mg iodoacetamide instead of DTT. The second dimension, which used PROTEAN II xi Cell (Bio-Rad, Hercules, CA), was performed using 12% SDS-PAGE at 20 mA/block for nearly 4 h, until the dye front reached the end of the gel. Gels were stained with Coomassie Brilliant Blue (CBB) G-250 according to Candiano et al.²² A total of 108 2-DE gels containing the samples from three regions of the internode (base, middle and top) under four developmental stages with three sample replicates and three experimental replicates each were analyzed.

Images of the stained gels were captured with a scanner (UMAX Powerlook 2100 XL; UMAX, Taiwan, China) and analyzed with ImageMaster 2D Platinum Software (Version 6.0; Amersham Biosciences, Uppsala, Sweden). Spot detection, matching, and background subtraction were performed using this software, followed by manual editing. All the spots detected in each gel were matched with the corresponding spot in reference gels. To eliminate differences arising from unequal sample loading or in gel staining and destaining, the normalized relative percent volume values (% volume) of the protein spots in triplicates of each sample were subjected to further statistical analysis. For visualization of differential protein expression in the different internodes (basal, middle, top) and in the different developmental stages (G1, G4, G7 and G9), gels of two given internodes in the same developmental stage or two given developmental stages in the same internode were grouped and all groups were analyzed with Student's *t* test. Differentially expressed spots were selected for further analysis if they displayed at least a 2-fold change in % volume and a *P* value <0.05.

MALDI-TOF/TOF MS

Selected spots were excised manually from the 2-DE gels and digested following the method described by He et al.²³ MS analysis was performed according to the method of Cui et al. with some modifications,²⁴ using a MALDI-TOF/TOF tandem mass spectrometer ABI 4800 proteomics analyzer (MALDI-TOF/TOF mass spectrometer, Applied Biosystems, Framingham, MN). For acquisition of mass spectra, 0.4 μ L samples were spotted onto a MALDI plate, followed by 0.4 μ L matrix solution (10 mg/mL CHCA in 50% ACN and 0.05% TFA). Mass data were acquired with 4000 Series Explorer Software v3.5 in batch-processing mode of MS/MS. All MS survey scans were acquired over the mass range *m/z* 800–4000 in the reflection positive-ion mode. The MS spectra were externally calibrated using Calibration Mixture 5 (Applied Biosystems) (*m/z* 904.468, 1296.685, 1570.677, 2093.087, 2465.199 and 3657.929) resulted in mass calculation errors of <5 ppm. The MS peaks were detected on minimum S/N ratio \geq 10 and cluster area S/N threshold \geq 40 without smoothing and raw spectrum filtering. Peptide precursor ions corresponding to contaminants including keratin and the trypsin autolytic products were excluded in a mass tolerance of 0.5 Da. Ten strongest filtered precursor ions with a user-defined threshold (S/N ratio \geq 50) were selected for the MS/MS scan. Fragmentation of precursor ions was performed using MS/MS 2 kV positive mode. The MS/MS spectra were calibrated using Glu1-Fibrinopeptide B (Applied Biosystems) (*m/z* 175.119, 684.346, 813.389, 1056.475 and 1441.634) resulted in mass errors of less than 20 ppm.

The MS/MS peaks were detected on minimum S/N ratio \geq 10 and cluster area S/N threshold \geq 20.

Database Search

For protein identification, the acquired MS and MS/MS data were uploaded on the Protein Pilot software v3.0 (Applied Biosystems, Framingham, MN) and compared against NCBI non-redundant protein sequence database (NCBI-nr) and Swiss-Prot database (released on May, 2010). Search parameters used were as follows: one missed cleavage per peptide; fixed modification, carboxymethyl; variable modifications, oxidation; monoisotopic mass; enzyme, trypsin; taxonomy, green plants; precursor ion mass tolerance, 100 ppm; MS/MS fragment-ion mass tolerance, 0.4 Da. Top ten hits for each protein search are reported.

The identified sequence tags were accepted when their MOWSE (molecular weight search) scores exceed the threshold (>71 for NCBI-nr or >59 for Swiss-Prot). Meanwhile, it had more than one peptide matched and a nearly complete y-ion series and complementary b-ion series present. In addition, the identified sequence tags that exceed the threshold and had only one peptide matched were also accepted, given the scarcity of relevant information available for Moso bamboo. A stringent threshold was applied to filter MS/MS peak (i.e., minimum S/N ratio \geq 10 and cluster area S/N threshold \geq 20). If a protein spot matched different proteins in different databases or matched multiple members of a protein family, then the number of matching peptides, the coverage, as well as pI and mass value nearest to the observed one were taken into consideration for establishing the identity.

Immunoblot Analysis

Protein samples were originated from mixed sample with three biological replicates. Protein samples (10 μ g) were separated on 10% SDS-PAGE and then transferred onto a PVDF membrane (wet transfer). The blotted membrane was blocked overnight at 4 °C in TBS buffer (20 mM Tris-HCl, 137 mM NaCl) containing 5% (w/v) nonfat dry milk and 0.2% Tween. The membranes were rinsed with TBS and subsequently incubated with polyclonal antibodies of antielongation factor 1-delta 1 (AS10 677, Agrisera, Sweden), actin 11 (AS10 702, Agrisera, Sweden), UDP-glucose pyrophosphorylase (AS05 086, Agrisera, Sweden), Fructose-bisphosphate aldolase (LKY001, ABMAX, China) and S-adenosylmethionine synthetase (LKY002, ABMAX, China) at 1:2000 dilution for 2 h at room temperature. After incubation with horse radish peroxidase (HRP) conjugated secondary antibodies for 1 h, the cross-reacting bands were detected with chemiluminescent (ECL) substrates.

Statistical Analysis

Student's *t*-test was used to select the spots for which the stage had a significant effect. One-way ANOVA and least significant difference (LSD) test were used to check for differences in cell morphology. *P* \leq 0.05 was considered as statistically significant.

RESULTS

Anatomical Variation in Different Developmental Stages of the Internodes

Internode tissue samples were collected (Figure 1) and observed under the microscope. The transverse and longitudinal sections revealing the vascular and parenchyma cells in the same developing internode were compared during different developmental stages (Figure 2A and B). In the initial stage of growth, numerous cell nuclei could be seen in parenchyma and

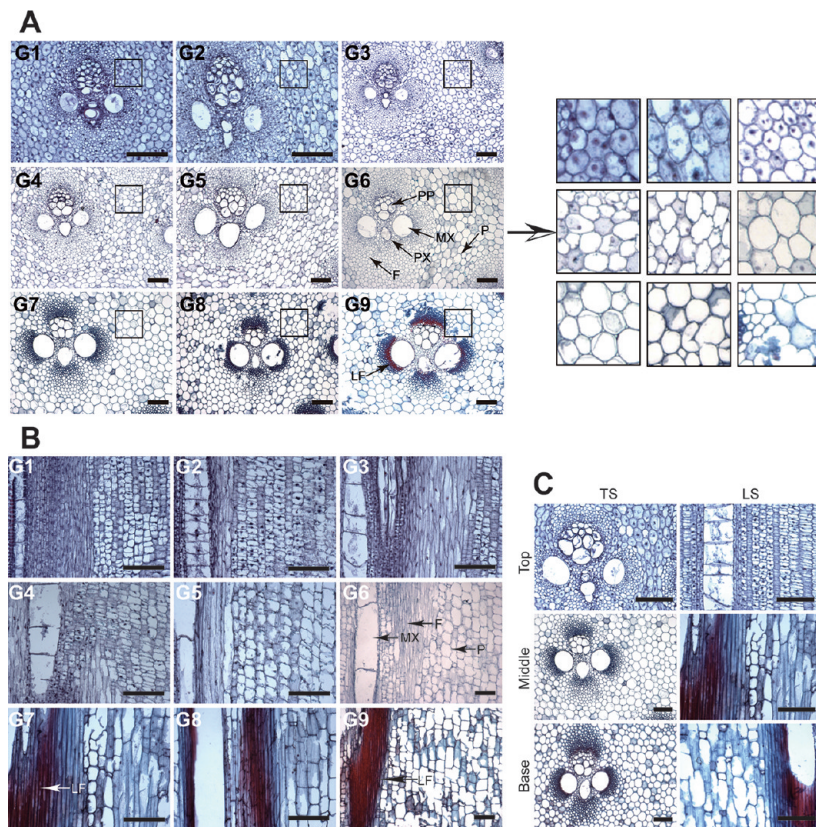


Figure 2. Anatomical observation of culm development of *P. heterocycla*. (A) Transverse section (TS) of tissue from the same developing internode (middle internode shown here) in nine developmental stages (G1–G9). The areas of black box were enlarged to display in the right panel. (B) Longitudinal section (LS) of a similar area from each developmental stage. (C) TS and LS of tissue at three developmental internodes in the same developmental stage (G7 shown here). Base, Middle and Top represent basal, middle and top internodes, respectively. Arabic numerals in the top left corner of picture indicate the developmental stage. CN, cell nuclei; F, fiber cells; LF, lignification of fiber cells; MX, metaxylem; P, parenchyma cells; PP, protophloem; PX, protoxylem. Scale bars: 100 μ m.

fiber cells—an obvious sign of cell division—indicating the presence of meristematic tissue. As the culm developed, the number of nuclei declined, until there were almost no detectable nuclei in the late stages of development. Meanwhile, the length of parenchyma and fiber cells increased continuously during the development. In addition, lignification of fiber cells occurred after the seventh developmental stage. Comparison of transverse and longitudinal sections of three developing internodes in the same developmental stage (Figure 2C) indicated that the number of nuclei in the tissue increased continuously from basal internode to top internode, while the cell length showed the opposite trend.

Usually, internode elongation is correlated with cell division and elongation. The dynamic changes of cell length and number of cell nuclei within a tissue were a direct evidence of cell elongation and division. The cell length of the same internodes during different stages showed a significant increase ($P < 0.05$) (Figure 3), which is particularly evident in the middle internode. On the contrary, rate of occurrence of cell nuclei presented a decreasing tendency in successive developmental stages. The cell length decreased from basal internode to top internode before the seventh developmental stage. The above results showed that cell division and cell elongation occurred simultaneously affecting internode elongation and that the former was predominant in initial stages, while the latter was predominant in late stages. Thus, the culm showed sequential

development from basal internode to top internode throughout the growth period.

Variation of Endogenous Hormones during Different Developmental Stages

The dynamic changes in ZR concentration of the three developmental internodes all displayed a bimodal type. The first peak of three developmental internodes all appeared at G3, whereas the second peak of basal, middle and top internodes appeared at G7, G8 and G6, respectively. During the developmental stage, ZR concentrations of the top internode were always higher than that of basal internode. In early stages (G1–G3), the ZR concentration increased from basal to top internode, which changed with growth (Figure 4A). The dynamic changes in GA₃ concentration of the three developmental internodes all generally displayed a bimodal type. The first peak of basal, middle and top internodes appeared at G5, G4 and G3, respectively, and the second peak of the three developmental internodes all appeared at G7 (Figure 4B). IAA concentration was high compared to the other three endogenous hormones in this study, which reached to microgram level. Similarly, the dynamic changes in IAA concentration of the three developmental internodes all displayed a bimodal type (Figure 4C). The dynamic changes in ABA concentration were obviously different from that of the above-mentioned hormones. In early stages (G1 and G2), the ABA concentration of the three developmental internodes maintained a high level and then decreased to a low level after G2 (Figure 4D).

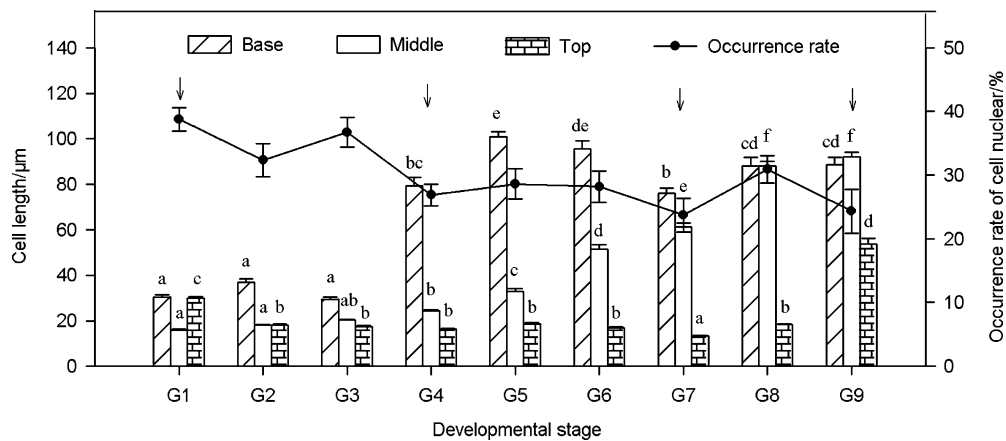


Figure 3. Variations in cell length and occurrence rate of cell nuclei in different developmental stages and internodes. To determine cell division and elongation at different developmental stages and internodes, the cell length and the number of cell nuclei in longitudinal section of tissue were measured by observation under a microscope. For each developmental internode in different stages, measurements were taken over more than 50 microscopy fields. Each data point of the fold line represents the mean of three developmental internodes. Different letters on the column with the same pattern indicate significant differences at $P \leq 0.05$ according to the LSD test. Bars represent SE ($n > 150$).

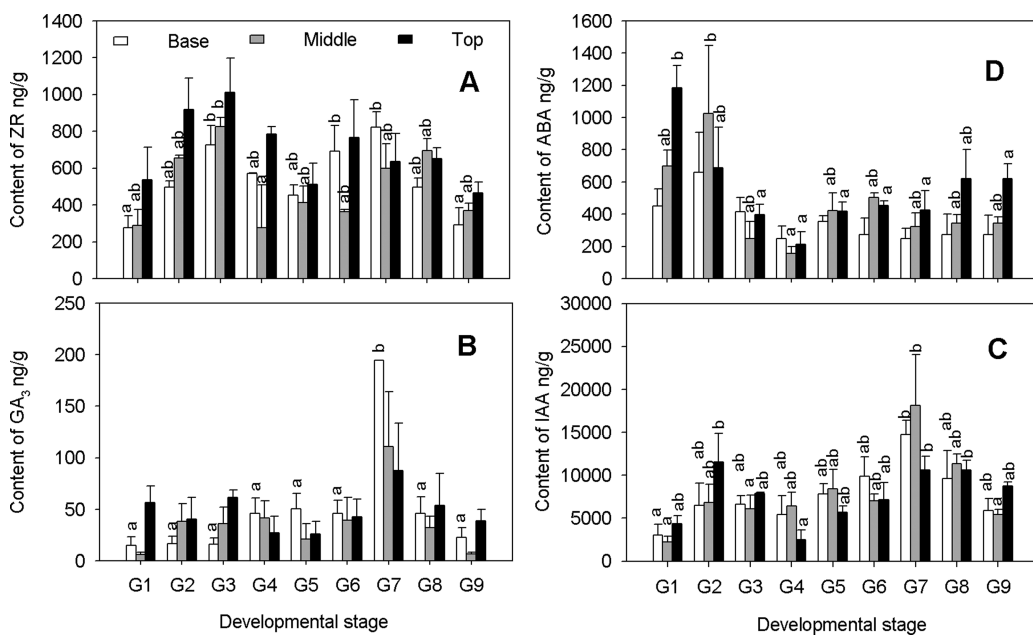


Figure 4. Changes in four endogenous hormones concentrations for *P. heterocyclo* culm at different developmental stages and internodes: abscisic acid (ABA), indole acetic acid (IAA), gibberellic acid (GA_3) and zeatin riboside (ZR). Each data point represents the mean of three biological replicates and three experimental replicates. Basal, middle and top represents the three internodes, and G1–G9 represent nine developmental stages. Different letters on a column with the same pattern indicate significant differences at $P \leq 0.05$ according to the LSD test. Bars represent SE ($n = 9$).

IAA, GA_3 , and ZR are often considered as growth promoting factors for plant development, while ABA is often regarded as an inhibitory factor. The ratio between the growth promoting factor and the inhibitory factor were compared in nine developmental stages (G1–G9) and all showed two peaks (Figure 5). The stages G4, G7 and G9 corresponded to significant cell elongation of basal, middle and top internode, respectively. This indicates that endogenous growth promoting hormones strongly influenced cell elongation. Therefore, samples of G1, G4, G7 and G9 were selected for further proteomic analysis.

Protein Reference Maps during Different Developmental Stages and Internodes

To obtain high quality and reproducible protein profiles of various samples, experimental conditions such as protein extraction and

solubilization methods, IEF conditions, and gel staining methods were optimized in preliminary experiments. A standardized protocol was established to produce protein expression maps with high reproducibility, clear background, and high throughput (Figure 6). Protein concentration of samples ranged from 1.03 to 10.86 $\mu\text{g}/\mu\text{L}$ with a mean of $5.99 \pm 3.79 \mu\text{g}/\mu\text{L}$. Generally, the protein concentration from basal to top internodes were increased. The protein concentration increased in early stages (G4 or G7), and then decreased in terminal stage (G9). Also, the decrease of protein concentration in top internode displayed a time lag compared with basal and middle internodes (Figure S1, Supporting Information). This phenomenon might be related to sequential development of culm. The number of protein spots detected per gel ranged from 550 to 1270 with a mean

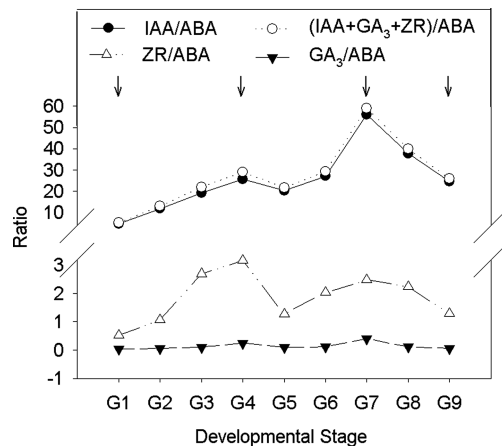


Figure 5. Ratio of four endogenous hormones in different developmental stages. Each data point represents the mean of three independent measurements of ratio of hormone levels, as indicated, in the three internodes (basal, middle and top) in the same developmental stage (G1–G9).

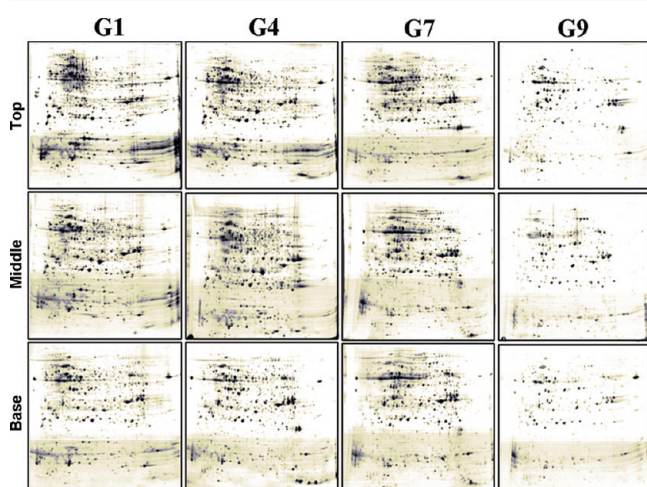


Figure 6. 2-DE maps of *P. heterocyclo* culm during the growth process. G1, G4, G7 and G9 represent different developmental stages. Base, middle and top represent basal, middle and top internode, respectively.

value of 957 ± 216 . There was a significant difference in the number of spots among different developmental stages (ANOVA, $P \leq 0.01$) but not significant in that among different developing internodes (ANOVA, $P \geq 0.05$), although significant differences in protein abundance were observed in both groups (ANOVA, $P \leq 0.01$). These data indicated that the protein expression varied more in response to the developmental stage and showed relatively less dependence on the location of the internode on the culm. In addition, cell elongation was possibly correlated with protein variation.

Protein Identification by MS/MS and Functional Categorization

The spot variations between the same internode in different developmental stages (G1, G4, G7 and G9) and those between different internodes (basal, middle and top) in the same developmental stage were analyzed. Two hundred fifty-eight reproducibly matched spots that showed at least a 2-fold change and displayed significant differences ($P < 0.05$) in abundance (Figure 7), were submitted for identification. Of these, 231 protein spots were successfully identified using MALDI-TOF/TOF

MS and database searches. Among the 231 proteins identified, 18 were rejected because they failed to match any peptide. There were 43 proteins that matched only one peptide and these were retained considering the scarcity of background information on *P. heterocyclo* sequences. Thus, a total of 213 proteins (Supplementary Table S1, Supporting Information) were analyzed and 77.5% of these were matched against gramineous species including rice (47.9%), wheat (3.3%), maize (17.4%), barley (1.9%), broomcorn (5.2%), and bamboo (1.9%), which is in accordance with the results of Cui et al.²⁴ Molecular weights ranged from 12 to 111 kDa and the pK_a ranged from 4.20 to 9.79.

The total of 213 differentially expressed proteins included 189 unique proteins and were divided into 11 categories according to Bevan et al.²⁵ (Figure 8A). Almost half of these belonged to two categories: metabolism and energy. On the basis of predicted subcellular location, these were classified into 13 categories, and about 45.4% of these were of unknown subcellular location (Figure 8B).

Stage-specific and Internode-specific Protein Expression

Among the 213 differentially expressed proteins, 9 proteins (8 unique proteins) for which a significant difference in abundance only appeared among different developing internodes in the same developmental stage were defined as internode-specific differential proteins (Figure S2, Supporting Information), while 175 proteins (155 unique proteins) for which difference in abundance only appeared among the different developmental stages in the same internode were defined as stage-specific proteins. In addition, 29 other proteins (26 unique proteins) for which significant difference in abundance appeared at both among different developmental internodes and among different developmental stages were defined as internode- and stage-dependent proteins (Table S1, Supporting Information). These data suggest that both stage-specific and internode-specific proteins influence the developmental variations and that the majority of variations resulted from the stage-specific differences. These proteins were further classified on the basis of function (Figure 8). Strikingly, the proportion of internode- and stage-dependent proteins involved in metabolism, energy, and transcription were remarkably high, compared with those of stage-specific proteins.

The differentially expressed proteins between any two stages or two internodes were classified according to their predicted function (Figure 8C). It was found that the number of the differentially expressed proteins increased temporally and spatially, and that temporal variations were more influential than the spatial ones. There were a few differentially expressed proteins before G7, but the number increased 10-fold after G7. Variations in the middle internode were more than those in the basal and top internodes. Regardless of temporal and spatial differences, the largest share of differentially expressed proteins was related to metabolism, energy, transcription, protein synthesis, and protein destination and storage.

Twenty-nine proteins (26 unique proteins) were defined as internode- and stage-dependent proteins (Figure S3, Supporting Information). Many of these showed a similar expression pattern: the abundance of these proteins was higher in the basal internode than in the middle and top internodes through G1 to G4. Subsequently, the abundance in the middle and top internode surpassed that in the basal internode through G7 to G9. These proteins were found to be related to polysaccharide biosynthesis (spots 49 and 58), fiber biosynthesis (spot 75), sucrose degradation (spot 138), TCA cycle (spot 123),

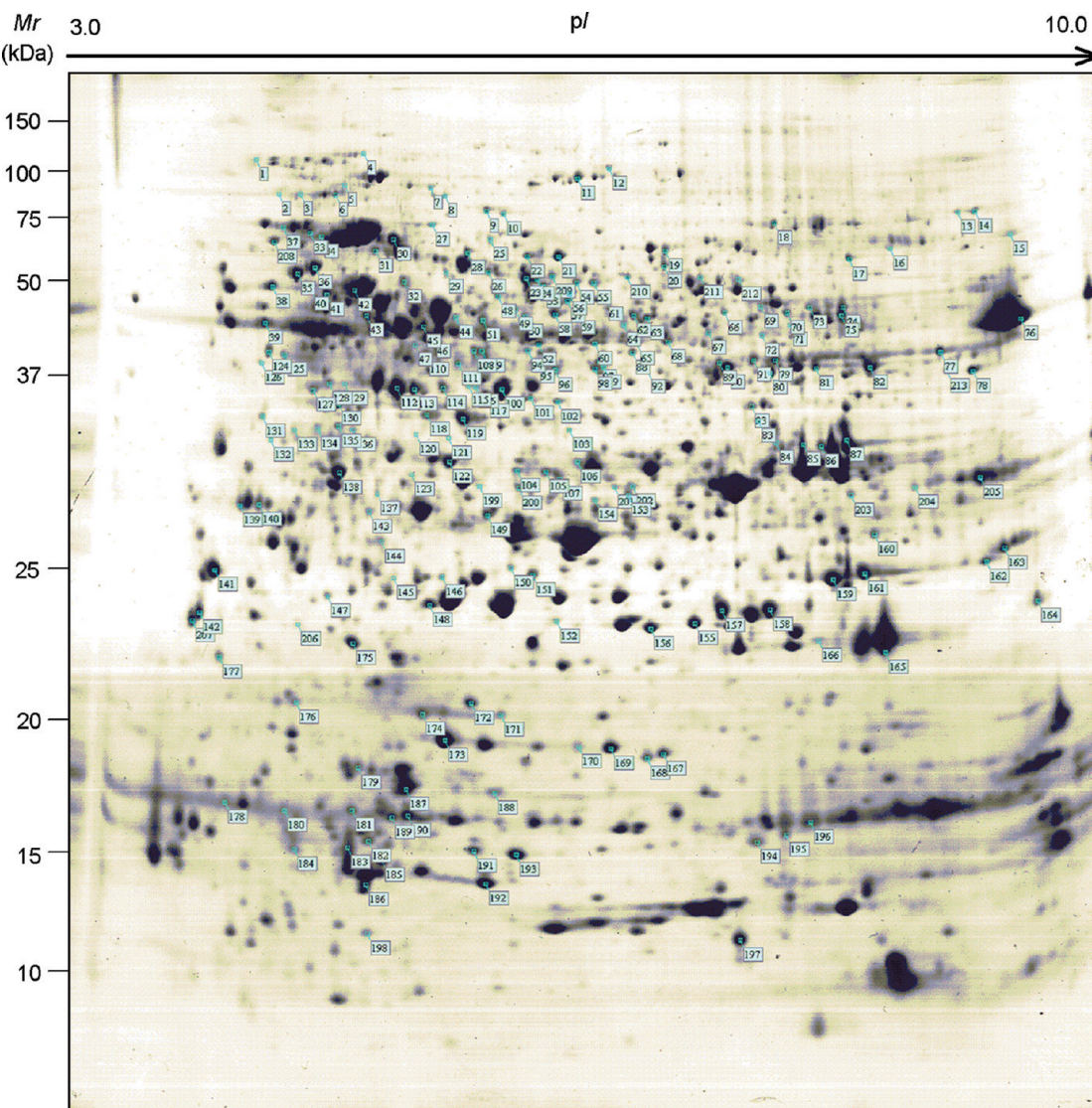


Figure 7. 2-DE map of *P. heterocyla* culms. The relative M_r (on the left) and the pI (on the top) are given. A total of 213 spots were successfully identified.

glycolysis (spots 71 and 146) and antioxidant enzyme (spot 203). In addition, the proteins related to photosynthesis (spots 134 and 205), transcription factors (spots 13, 55, 169 and 173), protein synthesis (spots 92, 165 and 185), and protein modification (spots 159 and 161) showed a higher abundance in tender tissues (middle or top internodes) than in mature tissues (basal internode). The above-mentioned were in accordance with the anatomical observations of the tissue sections and suggested that the sequential development from base to apex of culms was implemented by temporal and spatial expression of enzymes. The abundance of spot 117, involved in lipid biosynthesis, was higher in the basal internode than in other internodes during the developmental stage. Considering that basal internode matures first, we conjecture that the lipid biosynthesis might be related to the formation of epidermis cutin.

Dynamic Changes in Proteins Expressed Differentially during Development in Different Internodes

Based on the dynamic changes in proteins expressed at each internode in different stages five types of proteins could be distinguished: gradual increase (U-type), gradual decrease

(D-type), transitional increase (A-type), transitional decrease (B-type) and bimodal structure (C-type) (Figures 9 and S4, Supporting Information). The numbers of proteins of A-type and U-type from basal to top internodes were increased, in contrast to proteins of C-type. The kinetic changes of protein abundance at the three internodes were integrated. It is surprising that the proportion of the identified proteins whose abundance variation occurred synchronously at different internodes during the same developmental stages (i.e., AAA, DDD, CCC and UUU types) was only 14%, whereas 18.3% of proteins displayed a time lag in different internodes (e.g., DAA, AUU, DDA, AUU, AAU, DAU and CUU types). Interestingly, the kinetic changes of homologues were different. For example, although spots 49, 58, 59, 62, and 66 were all identified as UDP-glucose 6-dehydrogenase, spots 49 and 58 belonged to AAA type, spot 59 belonged to AUA type, spot 62 belonged to AAU type and spot 66 belonged to AAB type. The presence of protein isoforms with different expression patterns has been reported and these probably resulted from degradation products of the native protein^{26,27} or from post-translational modifications. These results suggested that there were extensive

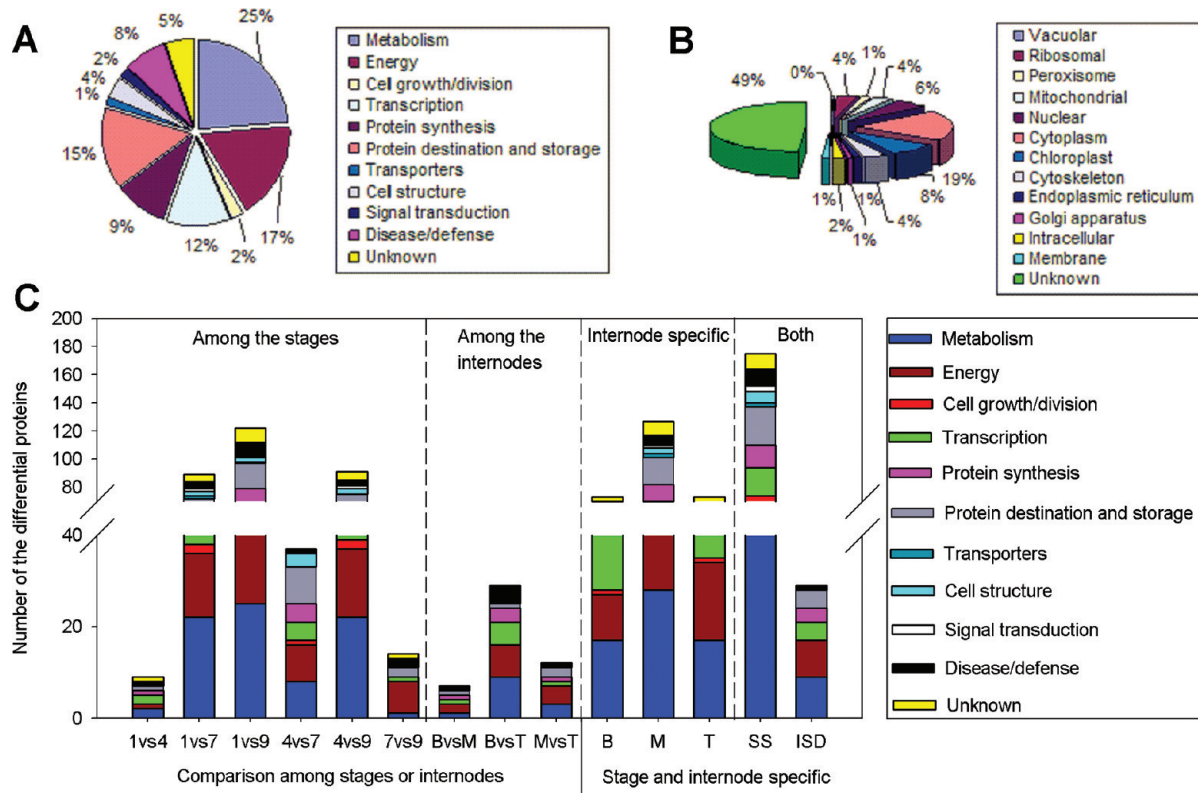


Figure 8. Classification of identified proteins. Classification based on (A) function, (B) subcellular location or (C) developmental stages and internodes. The localization and function prediction of proteins was based on the UniProt database (www.uniprot.org). In X-axis, B, M and T represent basal, middle and top internodes, respectively. 1, 4, 7, and 9 represent the four developmental stages (G1, G4, G7 and G9, respectively). SS indicates stage-specific differentially expressed proteins; ISD indicates internode and stage-dependent differentially expressed proteins.

temporal and spatial variations in protein expression during culm development.

Validation of Candidate Proteins by Immunoblot Analysis

In order to validate the proteomic results, elongation factor 1-delta (spot 139) involved in translational elongation, S-adenosylmethionine synthetase (spot 100) involved in synthesis of amino acids and hormones, Fructose-bisphosphate aldolase (spot 85) related to glycolysis, UDP-glucose pyrophosphorylase (spot 46) involved in synthesis of sucrose, cellulose and other saccharides, and actin related to cell skeleton of different developmental stages and internodes were further examined by immunoblot analyses using specific antibodies (Figure 10). The results showed that the molecular weight of cross-reacting bands corresponded to the expected values on SDS-PAGE. Accumulation differences at the corresponding developmental stages and internodes were confirmed for all analyzed proteins on the protein level, although the degree of variation between the 2-DE and immunoblot. In addition, actin 11 was not identified in the previous 2-DE and MS approached. However, it showed distinct expression among stages and internodes in immunoblot. This might be related to the fact that the resolution of 2-DE and success rate of protein identification by MS were limited.

DISCUSSION

Response of Dynamic Changes in Expression of Proteins to Endogenous Hormones

Plants rely on a diverse set of small-molecule hormones to regulate physiological processes, particularly growth.²⁸ Recent

studies on dwarf mutants have revealed that bioactive GAs regulate natural developmental processes including stem growth in plants.²⁹ It has been reported that succinate dehydrogenase (spot 210),³⁰ malate dehydrogenase (spot 123),³¹ 6-phosphogluconate dehydrogenase (spot 68)³² and S-adenosylmethionine synthetase (spots 100, 101, 115, 116 and 135) are involved in hormone biosynthesis. In this study, the dynamic changes in the expression of the above proteins appeared to be synchronized with the changes in hormone levels.

Expression Pattern of Differential Proteins in Rapidly Elongating Culms of *P. heterocycla*

The proteome variations of tomato (*Solanum lycopersicum*) pericarp development showed that amino acid metabolism or protein synthesis were mainly expressed during the cell division stage and down-regulated later. During the cell expansion phase, proteins associated to photosynthesis and proteins linked to cell wall formation transiently increased. The major part of the proteins related to carbon compounds, carbohydrate metabolism, oxidative processes and stress responses were up-regulated during fruit development, showing an increase in spot intensity during development and maximal abundance in mature fruits.^{33,34} During fiber development, the proteins involved in protein, amino acid and lipid metabolism reached higher volumes during the earlier elongation stages and declined during later stages. The cytoskeleton-proteins were also up-regulated.³⁵ These previous findings were generally consistent with our results. In addition, we found that the proteins involved in transcription showed decreases or transitional decreases.

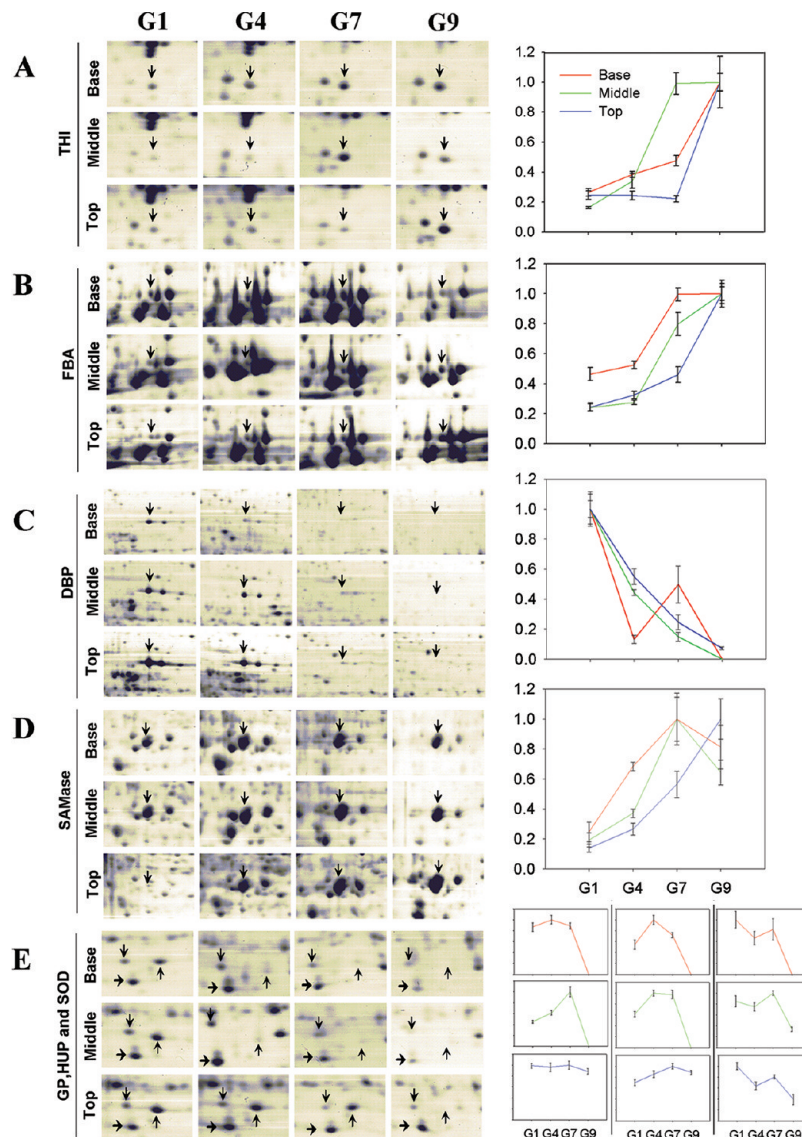


Figure 9. Patterns of differential protein expression in different developmental stages and internodes. Gel pictures and expression profiles of proteins are given in the left and right panels, respectively. In all line graphs, *x*-axis indicates four developmental stages (G1, G4, G7 and G9) and *y*-axis represents relative abundance of proteins. Base, Middle and Top represent basal, middle and top internode, respectively. The kinetic changes in protein abundance at each developmental internode in different stages are distinguished into five types: gradual increase during culm development (U-type), gradual decrease during culm development (D-type), those that showed initially increased and finally decreased abundance, with a single peak were defined as transitional increase (A-type), those that showed initially decreased and finally increased abundance, with a single valley were defined as transitional decrease (B-type), and those that had two peaks during culm development were defined as bimodal structure (C-type). After integrating kinetic changes in protein abundance at the three internodes, seven differential proteins were enumerated as follows: (A) THI, Thioredoxin (spot 198, UUU type). (B) FBA, Fructose-bisphosphate aldolase (spot 86, UUU type). (C) DBP, DNA-binding protein MNIB1B (spot 173, CDD type). (D) SAMase, S-adenosylmethionine synthetase 1 (spot 100, AAU type). (E) Three arrows from top to bottom counterclockwise are corresponding to GP-Glutathione peroxidase (spot 191, AAC type), HUP-Putative uncharacterized protein (spot 192, AAA type), SOD-Superoxide dismutase [Cu-Zn] (spot 193, CCC type). The small line plot of E from left to right correspond to spots 191, 192, and 193, respectively. Bars represent SE ($n = 9$).

Proteins Related to Carbohydrate and Amino Acid Metabolism in Rapidly Elongating Culms of *P. heterocyla*

Hexose derived from sucrose degradation was used to meet the energy requirements for growth and substrate requirements for the synthesis of fructans, starch, and cellulose.³⁶ Spot 138 was identified as fructokinase, which was linked to sucrose degradation, after conversion of β -D-fructofuranose and D-fructose-6-phosphate. The latter is the starting material for glycolysis.³⁷ It is reported that fructokinase plays a regulatory role in photosynthetic tissues, regulating photosynthesis, growth, and

senescence,³⁸ and that overexpression of fructokinase can inhibit the decline of adenylate energy status during prolonged hypoxia.³⁹ Fructokinase, in the present study, was up-regulated during the growth stage (Figure 11); in contrast, fructokinase showed a transitional increase during fiber elongation of cotton (*Gossypium hirsutum*).³⁵ Uridine diphosphoglucose, the substrate for cellulose synthesis, can be produced by cleavage of sucrose, as catalyzed by sucrose synthase (SuSy), or by phosphorylation of glucose-1-phosphate, as catalyzed by UDP-glucose pyrophosphorylase (UGP) (spot 46).⁴⁰ In addition, granule-bound starch synthase (spot 32) and alpha-1,4-glucan-protein

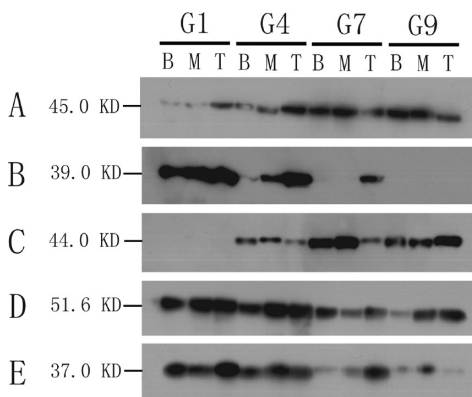


Figure 10. Immunoblot analysis of five proteins in different developmental stages and internodes. (A) Actin 11; (B) Fructose-bisphosphate aldolase; (C) S-adenosylmethionine synthetase; (D) UDP-glucose pyrophosphorylase; (E) elongation factor 1-delta 1. G1, G4, G7 and G9 indicate four developmental stages. B, M and T represent basal, middle and top internodes, respectively.

synthase (spots 118 and 119) participate in starch biosynthesis and cell wall biosynthesis. Spots 49, 58, 59, 62, and 66 were identified as UDP-glucose 6-dehydrogenase (UGD) that catalyzes the synthesis of UDP-glucuronate,⁴¹ which is an important polysaccharide in plant cell walls.^{42,43} The above-mentioned proteins are related to carbohydrate metabolism, except for spot 32, and were up-regulated coordinately. This indicated that continued sucrose degradation and synthesis of polysaccharide provided material resources for tissue formation during the development of bamboo.

Several proteins are involved in the synthesis of amino acids, including S-adenosylmethionine synthetase (SAMase) (spots 100, 101, 115, 116 and 135) related to methionine; anthranilate synthase component I family protein (spot 209) associated with tryptophan; a putative threonine synthase (spots 67 and 72) correlated with threonine; arginase (spot 103), argininosuccinate synthase (spot 96); a probable N-acetyl-gamma-glutamyl-phosphate reductase (spot 93) linked to arginine; and ketol-acid reductoisomerase (spots 48, 56, 57 and 61) related to isoleucine, valine and leucine. It is well established that methionine not only is a building block of protein biosynthesis but also occupies a central position in plant cell metabolism in which about 80% of methionine converts into SAM via SAMase. Furthermore, the resulting metabolite SAM is the major methyl-group donor in transmethylation reactions and an intermediate in the biosynthesis of polyamines and of the phytohormone ethylene.⁴⁴ In the present paper, five isoforms of SAMase displayed different accumulation patterns, for example, spot 100 showed a gradual increase while spot 135 displayed a transitional increase.

Chorismate is an important intermediate that leads to the biosynthesis of several essential metabolites including aromatic amino acids, vitamins E and K, ubiquinone and certain siderophores.⁴⁵ Besides, the chorismate pathway is related to lignin biosynthesis.^{46–48} Spots 73, 74, and 75 were identified as isoforms of phospho-2-dehydro-3-deoxyheptonate aldolase, one of the enzymes involved in chorismate biosynthesis,⁴⁹ and all three were up-regulated during the development in bamboo. Patatin T5 precursor (spot 117), hypothetical protein OsJ_26466 (spot 170), 3-oxoacyl-[acyl-carrier-protein] synthase I (spot 98) are related to fatty acid biosynthesis. Spots 12 and 51, spot 91, spot 94, and spot 105 are involved in

biosynthesis of vitamins, pyrimidine, purine, and pigment, respectively. Spot 83, putative acetyl-CoA C-acyltransferase, is involved in fatty acid β -oxidation. It has been reported that the fatty acid β -oxidation has essential roles in the breakdown of reserve triacylglycerols and postgerminative growth before the establishment of photosynthesis.⁵⁰ The spot showed a transitional increase, indicating that the fatty acid oxidation is possibly a channel to obtain energy during culm development.

Proteins Associated with Energy Metabolism in Rapidly Elongating Culms of *P. heterocycla*

In plants under anoxic conditions, glycolysis is the predominant pathway fueling respiration. Many proteins identified were found to be enzymes of glycolytic pathway or sugar-phosphate metabolism: fructose-bisphosphate aldolase (spots 84, 85, 86, and 87), enolase (spot 110), NADP-dependent glyceraldehyde-3-phosphate dehydrogenase (spot 71), alcohol dehydrogenase (ADHs) (spots 89 and 90), putative phosphoglycerate mutase (spot 23), phosphoglycerate kinase (spot 114).⁵¹ These enzymes mainly showed gradual or transitional increases, suggesting that bamboo culm adopted glycolysis and fermentation as means of ATP production during culm development. Also, several up-regulated enzymes related to tricarboxylic acid cycle (TCA cycle) were observed, including malate dehydrogenase (spot 123), succinate dehydrogenase (spot 210), and putative aconitate hydratase (spot 11), implying that aerobic respiration was gradually taking over concomitant with the shedding of the culm sheath. Numerous previous papers have reported that several enzymes involved in glycolysis and the TCA cycle were associated with plant development.³⁴ For example, fructokinase,³³ malate dehydrogenase,⁵² glyceraldehyde 3-phosphate dehydrogenase,⁵³ aldolase, phosphoglycerate kinase,⁵³ enolase⁵³ and ADHs⁵⁴ were differentially expressed during fruit development and ripening. Furthermore, glyceraldehyde 3-phosphate dehydrogenase, phosphoglycerate mutase and enolase were differentially expressed in cotton fiber development.³⁵

In the present paper, there were a few differential proteins associated with photosynthesis. Two RuBisCO large subunit-binding protein (spots 40 and 41) and oxygen-evolving enhancer protein (spot 144) were also detected, which mainly showed gradual increases. In view of their low quantity and abundance, we speculate that photosynthetic capacity of bamboo culm during the whole development period was weak, and that the photosynthetic capacity gradually strengthened from early to late stages. While some proteins related to oxidative phosphorylation were up-regulated, including the 75 kDa subunit of NADH-ubiquinone oxidoreductase (spots 9 and 10), ATPase (spots 43, 45 and 182), and thioredoxin (spot 198). This indicates that bamboo culm possessed some photosynthetic capacity before leaf expansion, but most of the energy was derived from heterotrophic metabolism. Three down-regulated enzymes, NADPH producing dehydrogenase of the oxidative pentose phosphate pathway (spot 60) and 6-phosphogluconate dehydrogenase (spots 65 and 68), were linked to pentose phosphate pathway that is necessary to form pentose and NADPH, indicating that these enzymes mainly play a role in the early development stage of bamboo culm.

Proteins Associated with Protein Synthesis in Rapidly Elongating Culms of *P. heterocycla*

In eukaryotes, the nucleosome is the basic unit of chromatin and is composed of four types of core histones.⁵⁵ Covalent modifications of the N-terminal tails of the core histones play pivotal roles in chromatin remodeling and in gene regulation.⁵⁶

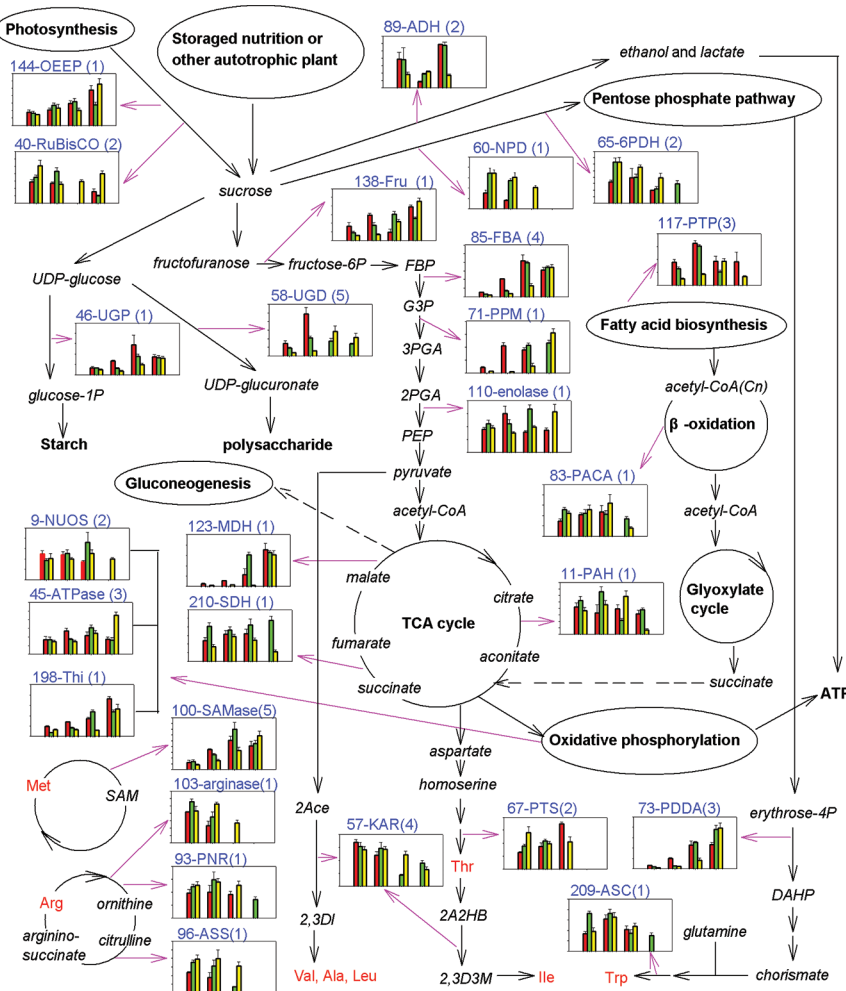


Figure 11. Changes in cellular metabolites and energy metabolism during the culm development of *P. heterocyclo*. Fold changes in differential expression of proteins involved in metabolic pathway is represented by column charts ($n = 9$) and guided by pink arrows. The spot number in 2-DE, protein name, and the number of homologue are denoted by the digits, text, and digits in brackets, respectively, above each column chart. The X- and Y-axes of the column charts represent four developmental stages (G1, G4, G7 and G9) and %volume, respectively. Red, green and yellow column indicate basal, middle and top internode, respectively. Pathways shown are based on resource of AraCyc. 2,3D3M, 2,3-dihydroxy-3-methyl; 2,3DI, 2,3-dihydroxy-isovalerate; 2A2HB, 2-aceto-2-hydroxy-butanoate; 2Ace, 2-acetolactate; 2PGA, 2-phosphoglycerate; 3PGA, 3-phosphoglycerate; 6PDH, 6-phosphogluconate dehydrogenase; ADH-alcohol dehydrogenase; ASC, anthranilate synthase component I family protein; ASS, argininosuccinate synthase; DAHP, 3-deoxy-D-arabino-heptulosonate-7-phosphate; FBA, fructose-bisphosphate aldolase; FBP, fructose-1,6-bisphosphate; Fru, fructokinase; G7P, glyceradehyde-3-phosphate; KAR, ketol-acid reductoisomerase; MDH, malate dehydrogenase; NPD, NADPH producing dehydrogenase of the oxidative pentose phosphate pathway; NUOS, NADH-ubiquinone oxidoreductase 75 kDa subunit; OEEP, oxygen-evolving enhancer protein; PACA, putative acetyl-CoA C-acyltransferase; PAH, putative aconitate hydratase; PDDA, phospho-2-dehydro-3-deoxyheptone aldolase; PEP, phosphoenolpyruvate; PNR, probable N-acetyl-gamma-glutamyl-phosphate reductase; PPM, putative phosphoglycerate mutase; PTP, Patatin T5 precursor; PTS, putative threonine synthase; RuBisCO, RuBisCO large subunit-binding protein subunit; SAMase, S-adenosylmethionine synthetase; SDH, succinate dehydrogenase; Thi, Thioredoxin; UGD, UDP-glucose 6-dehydrogenase; UGP, UDP-glucose pyrophosphorylase.

Spot 178 was identified as a probable histone and was down-regulated. Nucleotide excision repair (NER) is a light-dependent mechanism of DNA repair, recognizing and resolving a variety of helix-distorting lesions.⁵⁷ Spots 8, 124, 125, and 126 were related to NER and showed transitional increases or decreases. These proteins must contribute to the rapid cell growth and division in the initial developmental stage, and their relative abundance declined along with slowing of the cell growth/division as the tissue matured, which was consistent with the anatomical data. Spot 177 was identified as a RNA-binding glycine-rich protein (GRPs) involved in plant responses to changing environmental conditions.⁵⁸ Mangeon et al.⁵⁹ reported that AtGRPS, a vacuole-located GRP, was involved in organ growth by cell elongation processes in *A. thaliana*. Liu et al.⁶⁰ demonstrated that the

DNA-binding protein MNB1B was related to senescence of rice leaves. There was abundant DNA-binding protein MNB1B (spot 173) of down-regulated type. The transcription factor, GAMYB protein, induces the expression of α -amylase and some other GA-inducible genes by interacting directly with the GA-responsive cis-acting elements of these genes in the aleurone tissue,⁶¹ and may be involved in other GA-regulated events, such as floral organ development, pollen development, stem elongation, anther development, and seed development.^{62,63} Spot 13 (DDA type) and spot 14 (DAA type) were identified as putative GAMYB-binding protein, which indicates that starch degradation declined between the initial and the late stages, and between the basal and the top internodes. Spots 167, 168, 169, and 172 were identified as transcription factor BTF3, which is related to

apoptosis.⁶⁴ It has been reported that virus-induced gene silencing of NbBTF3 in *Nicotiana benthamiana* caused leaf yellowing and abnormal leaf morphology, and reduced the chloroplast size and chlorophyll contents.⁶⁵ In addition, some proteins (spots 4, 24, 26, 38, 47, 55, 78, 95, 102, 160, 177, 179, 186, 212 and 213) related to nucleotide binding (including DNA binding, RNA binding and RNA recognition) were identified, of which a majority were down-regulated.

Many proteins related to protein synthesis were identified, including six eukaryotic translation initiation factors (eIFs) (spots 27, 106, 165, 181, 189 and 190), five elongation factors (EFs) (spots 76, 139, 140, 199 and 211) and six ribosomal proteins (spots 122, 133, 164, 174, 185 and 197). Three-fifths of eIFs identified here were eIF5A, four-fifths of EFs were EF1, and five-sixths of ribosomal proteins were 40S ribosomal protein. There is a large body of literature on these proteins. eIF-5A does not act as a conventional translation initiation factor because it seems not to be required for global protein synthesis, but appears to function as a nucleocytoplasmic shuttle protein. It is known to be activated posttranslationally by modification of Lys into the unusual amino acid hypusine and is thought to play a determinant role in the translation of mRNAs required either for cell division or cell death.⁶⁶ Feng et al. found that eIF-5A2, in *Arabidopsis*, is critical for plant growth and development as it regulates cell division, cell growth, and cell death.⁶⁷ Three isoforms of eIF-5A (spots 181, 189 and 190) were identified. The high expression of these proteins was mainly displayed at early developmental stages (G1 and G4), and was subsequently down-regulated (G7 and G9). Especially, in the terminal developmental stage (G9), the expression of eIF-5A almost vanished. This tendency was consistent with EFs and ribosomal proteins. Zanelli et al. revealed that eIF-5A, in yeast, physically interacts with protein components of the translational machinery components, not only with structural components of the ribosome, but also with elongation factors, suggesting that eIF-5A specifically binds to actively translating ribosomes.⁶⁸ The above-mentioned, combined with the present results of tissue sections, elucidated that the interaction of eIF-5A, EFs and ribosomal protein possibly play a dominant role in cell division of *P. heterocycla*.

Also, importin α has been shown to interact with the cytoskeleton and could inactivate spindle formation during mitosis. Spot 42 was identified as importin subunit alpha-1b, which is involved in nuclear transport and plays fundamental roles in cell biogenesis and regulation of gene expression.^{69,70} Its abundance gradually decreased during culm development, which implied that it was involved in cell division of *P. heterocycla*. Spot 141 corresponded to nascent polypeptide-associated complex (NAC) alpha subunit-like protein and was down-regulated. The NAC is a heterodimeric complex that can reversibly bind to the eukaryotic ribosome,⁷¹ and is presumed to prevent ribosome-associated nascent polypeptides from inappropriate interaction with proteins in the cytosol.⁷² Chitteti et al.⁷³ demonstrated that the NAC might be involved in cell dedifferentiation, which is a cell fate switching process in which a differentiated cell reverts to a status with competence for cell division and organ regeneration. Some studies reported that NAC was down-regulated, for example in rice (*Oryza sativa*) roots,⁷⁴ and in sugar beet (*Beta vulgaris*) leaves⁷⁵ in response to stress. Furthermore, spots 92 and 121 were identified as Os07g0180900 and appeared to be up-regulated. It might be related to the function of translation as a structural component of ribosome.⁷⁶

Bamboo shoots after spring rain, a Chinese proverb, indicates that the bamboo growth rate is incredible and hints that development of bamboo is closely related to water uptake. Actually, the bamboo culm enlarges almost solely by cell expansion, which requires cell wall elongation and accumulation of solutes within the vacuole. Vacuolar H⁺-ATPase is a multimeric enzyme that contributes to the generation of the proton gradients across the tonoplast. V-ATPase is necessary for vacuolar acidification and for sorting of soluble proteins, such as vacuolar invertase, and can also promote cell growth by playing a role in membrane fusion events and exocytosis of wall material.^{33,77} In analysis of the proteome of tomato pericarp, expression of H⁺-ATPase was enhanced during the cell enlargement phase.³³ Our results showed that the abundance of V-type proton ATPase subunit B2 (spot 43) gradually increased during the developmental stage, indicating that it played a vital role in cell expansion of *P. heterocycla* culm. Adenosine kinase catalyzes the salvage synthesis of adenine monophosphate (AMP) from adenosine and ATP, and thereby contributes to the maintenance of cellular energy charge and to the synthesis of a variety of biomolecules, including nucleotide cofactors and nucleic acids.⁷⁸ Spot 130, an adenosine kinase isoform 2T, gradually increased during the developmental stage, consistent with proteomic analysis of the development of tomato pericarp and cotton fiber.

Some spots were identified as proteins involved in protein sorting, protein folding (spots 2, 3, 6, 20, 29, 30, 35, 36, 104, 147, 175 and 196), proteolysis (spots 7 and 52), protein degradation (spots 79, 81, 82, 149, 171, and 197) or post-translational modifications (spot 195). In addition, heat shock protein (HSP 70) (spots 5, 28, 33 and 37) that is considered as a molecular chaperone was also detected. In leguminous plants, storage proteins and starch are hydrolyzed in cotyledons and transported to growing stems and leaves, which rely on these reserves until photosynthetic tissue becomes functional. Mason et al.⁷⁹ discovered that in soybean, the mRNA for these proteins is most abundant in the stem region which contains dividing cells, less abundant in elongating and mature stem cells, and rare in roots. Spot 153 (putative legumin) and spot 208 (protein disulfide isomerase-like 1–4), for which expression pattern showed a tendency for up-regulation during development, plays a role in storage protein biogenesis. This suggests that in the developing bamboo culm, consumption of storage nutrients occurred before leaf expansion while small amounts of nutrients were stored for the next developmental stage. Microtubules are dynamic heteropolymers of α - and β -tubulin that assemble cocrateinately in response to a variety of intracellular and extracellular signals and participate in a number of different functions in eukaryotic cells, from cell division to organelle transport, from RNA positioning to flagellar beating.⁸⁰ The eukaryotic actin cytoskeleton plays a pivotal role in many cellular processes that together regulate cell growth and morphology.⁸¹ Eight proteins involved in microtubule and cytoskeletal activity were identified and their expression principally increased or transitionally increased during culm development.

Proteins Involved in Stress Response in Rapidly Elongating Culms of *P. heterocycla*

Plants lack a circulatory system to mobilize oxygen to heterotrophic roots, tubers, meristems, germinating pollen, and developing seeds. At the cellular level, a common eukaryotic response to oxygen deficiency is the Pasteur effect, whereby

glycolysis and fermentation are promoted and the TCA cycle and mitochondrial respiration are repressed.⁸² It is not surprising that organisms can be predisposed to endure or avoid a low-oxygen environment. For example, submergence-tolerant rice varieties adopt a quiescence strategy that limits the consumption of energy reserves and growth when covered by deep floodwaters,⁸³ whereas deepwater rice varieties that experience a progressive deep flood during establishment can accelerate elongation growth to extend leaves above water.¹⁰

It has been reported that plants are not only able to achieve a high degree of control over H₂O₂ toxicity, but also use H₂O₂ as a signaling molecule.⁸⁴ Loosening of plant cell walls, the most important reaction in the cell elongation process, is not only initiated by expansins,⁸⁵ as ROS (such as superoxide radicals, H₂O₂ and hydroxyl radical) were also found to participate in plant cell elongation.^{86,87} Yang et al.³⁵ indicated that H₂O₂ mediated cell expansion during cotton fiber elongation. In the rapidly growing bamboo culm, a large amount of reactive oxygen species are likely to be produced due to long-term anaerobic respiration. Many homologues of antioxidant enzymes were identified, including superoxide dismutase SOD [Cu-Zn] (spot 193), peroxide dismutase (POD) (spots 180, 191 and 203), catalase (CAT) (spots 69 and 70), glutathione S-transferase (spots 157 and 158). Four isoforms of SOD and POD showed a high abundance from G1 to G7, and declined in G9. Two isoforms of CAT and two isoforms of glutathione S-transferase gradually increased from G1 to G9. Our results suggested that ROS possibly regulated bamboo culm development.

Universal stress protein (USP) homologues appear to be ubiquitous in plants. Sauter et al.⁸⁸ indicated expression of OsUsp1 in the youngest internode of deepwater rice, which encodes a homologue of the bacterial USP family. Its expression was very strongly induced within 1 h of submergence. Elevated transcript levels were observed in dividing cells, in expanding cells and in differentiated tissue indicating that USP1 mediates a general process. Here, spot 131 was identified as a USP family protein and its abundance mainly decreased from G1 to G9, which is in accordance with the result of Sauter et al. This showed that the USP protein might play a role in plant growth in anaerobic environment. Spots 21, 22, 132, 183, and 184 were identified as stress-induced protein, which showed different expression patterns, and their role awaits further study.

Substance and Energy Metabolism Model for Rapidly Elongating Culms of *P. heterocyla*

Based on all the above results, we propose a model for the mechanism in rapidly growing culm of Moso bamboo (Figure 11): during all the developmental stages of the bamboo culm (from G1 to G9), the material for tissue construction mainly derived from storage nutrients and other autotrophic mechanisms, as the photosynthetic system was not yet functional. In the early developmental stages (G1 and G4), the culm was covered with a layer of culm sheath, which generates an anaerobic environment. During these stages, storage nutrients were degraded into monosaccharides and participated in anaerobic respiration to produce energy, while the aerobic respiration (i.e., TCA cycle, pentose phosphate pathway) played a minor role in generation of energy. Several transcription factors and molecular chaperones, and some biomacromolecules (e.g., protein, nucleic acid, polysaccharide, and lipid) were produced promoting generation of energy to support processes of cell division, cell elongation, tissue formation, and tissue maturation. In the anaerobic environment, levels of many antioxidant

enzymes were increased for scavenging free radicals, which ensures uninterrupted plant growth.

The anaerobic respiration became weak gradually after the culm sheath was shed in the later developmental stage (G9) and the TCA cycle became the major source for energy. As the existing sugars could not meet the demands of growth, a part of lipid that came from storage nutrition or from new synthesis was transformed into sugar through the β -oxidation and glyoxylate cycle. These vigorous early metabolic activities appeared at the basal internode, and with time the middle and top internode became sthenic progressively. In the stage G7, the observed increasing metabolic activity was related to the formation of pyruvate (fructose-bisphosphate aldolase, spots 84, 85, 86, and 87; enolase, spot 110; NADP-dependent glyceraldehyde-3-phosphate dehydrogenase, spot 71; putative phosphoglycerate mutase, spot 23; phosphoglycerate kinase, spot 114) and TCA cycle (malate dehydrogenase, spot 123; succinate dehydrogenase, spot 210; putative aconitate hydratase, spot 11). These data indicate that the shedding of culm sheath allowed a better access to oxygen, thus promoting the respiratory metabolism.

Also, proteins involved in anaerobic respiration (alcohol dehydrogenase, spots 89 and 90) decreased in abundance from the basal internode to the top internode in each developmental stage, and proteins related to TCA cycle (spots 11, 210, and 123) showed highest abundance in the middle internode in each developmental stages. Thus, the middle internode appears to generate more energy to implement the tissue construction than the basal and top internodes. It is possible that the mode of energy production of the middle internode is more efficient and may be correlated with the observation that the length of the middle internode is longer than that of basal and top internodes in a mature bamboo culm.

We provided an overview of culm development in Moso bamboo from a macromolecular level to further understand the developmental mechanisms. However, there were inherent shortcomings in the analysis of 2-DE data including a lack of accuracy in the quantitative analysis of proteins and the need for subjective judgment by the experimenter in the selection of differential proteins. Also, culm development is a complicated process involving numerous factors. Thus, a single experimental technique cannot provide a comprehensive picture. In the near future, more extensive studies with higher resolution techniques for protein separation and more accurate quantitative analysis methods, utilizing different methods based on systems biology will be necessary to validate some of the conclusions drawn here.

CONCLUSION

Moso bamboo culm is famous for its fast growth rate. To date, there have been no reports of protein expression profiling in a developing bamboo culm. The ratio of endogenous hormones was related to culm development. A total of 213 differential proteins were identified by MS. During the culm development, the proteins linked to amino acid metabolism, transcription and protein synthesis were mainly expressed during the cell division stage and down-regulated later, while the major part of the proteins related to carbohydrate metabolism, photosynthesis, oxidative processes, cytoskeleton and stress responses were up-regulated or transitionally increased. The sequential development from base to apex of the bamboo culm was implemented by temporal and spatial expression of proteins. During culm development, photosynthetic capacity was weak and most energy was derived from sucrose degradation. The shedding of the culm sheath played an important role in regulation of

anaerobic and aerobic modes of respiration. The rapid growth of Moso bamboo culm is closely related to differential expression of proteins involved in carbohydrate metabolism. This study provides a solid basis for understanding the growth and development of bamboo.

■ ASSOCIATED CONTENT

§ Supporting Information

Supplemental figures and table. This material is available free of charge via the Internet at <http://pubs.acs.org>.

■ AUTHOR INFORMATION

Corresponding Author

*Prof. Jianguo Zhang, Research Institute of Forestry, Chinese Academy of Forestry, Xiangshan road, Haidian District, Beijing 100091, People's Republic of China. Tel.: 86-10-62889601. Fax: 86-10-62872015. E-mail: zhangjg@caf.ac.cn.

Author Contributions

[†]These authors contributed equally to this work.

Notes

The authors declare no competing financial interest.

■ ACKNOWLEDGMENTS

This work was supported by the National Natural Science Foundation of China (30972332).

■ REFERENCES

- (1) Fu, J. H. Chinese moso bamboo: its importance. *Bamboo* **2001**, *22* (S), 5–7.
- (2) Magel, E.; Kruse, S.; Lütje, G.; Liese, W. Soluble carbohydrates and acid invertases involved in the rapid growth of developing culms in *Sasa palmata* (Bean) Camus. *Bamboo Sci. Cult.* **2006**, *19* (1), 23–29.
- (3) Jiang, Z. H. *Bamboo and Rattan in the World*; LiaoNing Science and Technology published House: China, 2007.
- (4) Peng, Z. H.; Lu, T. H.; Li, L. B.; Liu, X. H.; Gao, Z. M.; Hu, T.; Yang, X. W.; Feng, Q.; Guan, J. P.; Weng, Q. J.; Fan, D. L.; Zhu, C. R.; Lu, Y.; Han, B.; Jiang, Z. H. Genome-wide characterization of the biggest grass, bamboo, based on 10, 608 putative full-length cDNA sequences. *BMC Plant Biol.* **2010**, *10*, 116.
- (5) Lee, C. L.; Chin, T. C. Comparative anatomical studies of some Chinese bamboos. *Acta Bot. Sin.* **1960**, *9*, 76–95.
- (6) Murphy, R. J.; Alvin, K. L. Variation in fibre wall structure in bamboo. *Int. Assoc. Wood Anat. Bull.* **1992**, *13*, 403–410.
- (7) Lin, J. X.; He, X. Q.; Hu, Y. X.; Kuang, T. Y.; Ceulemans, R. Lignification and lignin heterogeneity for various age classes of bamboo (*Phyllostachys pubescens*) stems. *Physiol. Plantarum* **2002**, *114* (2), 296–302.
- (8) Luo, A. D.; Qian, Q.; Yin, H. F.; Liu, X. Q.; Yin, C. X.; Lan, Y.; Tang, J. Y.; Tang, Z. S.; Cao, S. Y.; Wang, X. J.; Xia, k.; Fu, X. D.; Luo, D.; Chu, C. C. *EUI₁*, encoding a putative cytochrome P450 monooxygenase, regulates internode elongation by modulating gibberellin responses in rice. *Plant Cell Physiol.* **2006**, *47* (2), 181–191.
- (9) Iwamoto, M.; Baba-Kasai, A.; Kiyota, S.; Hara, N.; Takano, M. *ACO1*, a gene for aminocyclopropane-1-carboxylate oxidase: effects on internode elongation at the heading stage in rice. *Plant Cell Environ.* **2010**, *33* (5), 805–815.
- (10) Hattori, Y.; Nagai, K.; Furukawa, S.; Song, X.; Kawano, R.; Sakakibara, H.; Wu, J.; Matsumoto, T.; Yoshimura, A.; Kitano, H. The ethylene response factors SNORKEL1 and SNORKEL2 allow rice to adapt to deep water. *Nature* **2009**, *460* (20), 1026–1030.
- (11) Zhou, H. L.; He, S. J.; Cao, Y. R.; Chen, T.; Du, B. X.; Chu, C. C.; Zhang, J. S.; Chen, S. Y. OsGLU1, a putative membrane-bound endo-1, 4- β -D-glucanase from rice, affects plant internode elongation. *Plant Mol. Biol.* **2006**, *60* (1), 137–151.
- (12) Asano, K.; Miyao, A.; Hirochika, H.; Kitano, H.; Matsuoka, M.; Ashikari, M. SSD1, which encodes a plant-specific novel protein, controls plant elongation by regulating cell division in rice. *Proc. Jpn. Acad., Ser. B* **2010**, *86* (3), 265–273.
- (13) Ruonala, R.; Rinne, P.; Kangasjarvi, J.; van Der Schoot, C. *CENL1* expression in the rib meristem affects stem elongation and the transition to dormancy in *Populus*. *Plant Cell* **2008**, *20*, 59–74.
- (14) Chen, C. Y.; Hsieh, M. H.; Yang, C. C.; Lin, C. S.; Wang, A. Y. Analysis of the cellulose synthase genes associated with primary cell wall synthesis in *Bambusa oldhamii*. *Phytochemistry* **2010**, *71*, 1270–1279.
- (15) Chiu, W. B.; Lin, C. H.; Chang, C. J.; Hsieh, M. H.; Wang, A. Y. Molecular characterization and expression of four cDNAs encoding sucrose synthase from green bamboo *Bambusa oldhamii*. *New Phytol.* **2006**, *170* (1), 53–63.
- (16) Hsieh, C. W.; Liu, L. K.; Yeh, S. H.; Chen, C. F.; Lin, H. I.; Sung, H. Y.; Wang, A. Y. Molecular cloning and functional identification of invertase isozymes from green bamboo *Bambusa oldhamii*. *J. Agric. Food Chem.* **2006**, *54* (8), 3101–3107.
- (17) Chen, T. H.; Huang, Y. C.; Yang, C. S.; Yang, C. C.; Wang, A. Y.; Sung, H. Y. Insights into the catalytic properties of bamboo vacuolar invertase through mutational analysis of active site residues. *Phytochemistry* **2009**, *70* (1), 25–31.
- (18) Zhou, M. B.; Yang, P.; Gao, P. J.; Tang, D. Q. Identification of differentially expressed sequence tags in rapidly elongating *Phyllostachys pubescens* internodes by suppressive subtractive hybridization. *Plant Mol. Biol. Rep.* **2010**, *29* (1), 224–231.
- (19) Wu, Y. J.; Chen, H. M.; Wu, T. T.; Wu, J. S.; Chu, R. M.; Juang, R. H. Preparation of monoclonal antibody bank against whole water-soluble proteins from rapid-growing bamboo shoots. *Proteomics* **2006**, *6* (22), 5898–5902.
- (20) Wang, Y.; Du, S. T.; Li, L. L.; Huang, L. D.; Fang, P.; Lin, X. Y.; Zhang, Y. S.; Wang, H. L. Effect of CO₂ elevation on root growth and its relationship with indole acetic acid and ethylene in tomato seedlings. *Pedosphere* **2009**, *19* (5), 570–576.
- (21) Bradford, M. M. A rapid and sensitive method for the quantitation of microgram quantities of protein utilizing the principle of protein-dye binding. *Anal. Biochem.* **1976**, *72* (1–2), 248–254.
- (22) Candiano, G.; Bruschi, M.; Musante, L.; Santucci, L.; Ghiggeri, G.; Carnemolla, B.; Orecchia, P.; Zardi, L.; Righetti, P. Blue silver: A very sensitive colloidal Coomassie G-250 staining for proteome analysis. *Electrophoresis* **2004**, *25* (9), 1327–1333.
- (23) He, C. Y.; Zhang, J. G.; Duan, A. G.; Zheng, S. X.; Sun, H. G.; Fu, L. H. Proteins responding to drought and high - temperature stress in *Populus × euramericana* cv.'74/76'. *Trees-Struct. Funct.* **2008**, *22* (6), 803–813.
- (24) Cui, S. X.; Hu, J.; Yang, B.; Shi, L.; Huang, F.; Tsai, S. N.; Ngai, S. M.; He, Y. K.; Zhang, J. H. Proteomic characterization of *Phragmites communis* in ecotypes of swamp and desert dune. *Proteomics* **2009**, *9* (16), 3950–3967.
- (25) Bevan, M.; Bancroft, I.; Bent, E.; Love, K.; Goodman, H.; Dean, C.; Bergkamp, R.; Dirkse, W.; Van Staveren, M.; Stiekema, W. Analysis of 1.9 Mb of contiguous sequence from chromosome 4 of *Arabidopsis thaliana*. *Nature* **1998**, *391*, 485–488.
- (26) Finnie, C.; Bak-Jensen, K. S.; Laugesen, S.; Roepstorff, P.; Svensson, B. Differential appearance of isoforms and cultivar variation in protein temporal profiles revealed in the maturing barley grain proteome. *Plant Sci.* **2006**, *170* (4), 808–821.
- (27) Sghaier-Hammami, B.; Valledor, L.; Drira, N.; Jorrin-Novo, J. V. Proteomic analysis of the development and germination of date palm (*Phoenix dactylifera* L.) zygotic embryos. *Proteomics* **2009**, *9* (9), 2543–2554.
- (28) Nemhauser, J. L.; Hong, F. X.; Chory, J. Different plant hormones regulate similar processes through largely nonoverlapping transcriptional responses. *Cell* **2006**, *126* (3), 467–475.
- (29) Sun, T. P. Gibberellin signal transduction in stem elongation & leaf growth. *Plant Horm.* **2010**, *308*–328.

- (30) Sekimoto, H.; Seo, M.; Dohmae, N.; Takio, K.; Kamiya, Y.; Koshiba, T. Cloning and molecular characterization of plant aldehyde oxidase. *J. Biol. Chem.* **1997**, *272* (24), 15280–15285.
- (31) Davey, M. W.; Van Montagu, M.; Inzé, D.; Sanmartin, M.; Kanellis, A.; Smirnoff, N.; Benzie, I. J. J.; Strain, J. J.; Favell, D.; Fletcher, J. Plant L-ascorbic acid: chemistry, function, metabolism, bioavailability and effects of processing. *J. Sci. Food Agric.* **2000**, *80* (7), 825–860.
- (32) Palma, J. M.; Corpas, F. J.; del Río, L. A. Proteome of plant peroxisomes: new perspectives on the role of these organelles in cell biology. *Proteomics* **2009**, *9* (9), 2301–2312.
- (33) Faurobert, M.; Mihr, C.; Bertin, N.; Pawlowski, T.; Negroni, L.; Sommerer, N.; Causse, M. Major proteome variations associated with cherry tomato pericarp development and ripening. *Plant Physiol.* **2007**, *143* (3), 1327–1346.
- (34) Palma, J. M.; Corpas, F. J.; del Río, L. A. Proteomics as an approach to the understanding of the molecular physiology of fruit development and ripening. *J. Proteomics* **2011**, *74* (8), 1230–1243.
- (35) Yang, Y. W.; Bian, S. M.; Yao, Y.; Liu, J. Y. Comparative proteomic analysis provides new insights into the fiber elongating process in cotton. *J. Proteome Res.* **2008**, *7* (11), 4623–4637.
- (36) Ciereszko, I.; Johansson, H.; Hurry, V.; Kleczkowski, L. A. Phosphate status affects the gene expression, protein content and enzymatic activity of UDP-glucose pyrophosphorylase in wild-type and pho mutants of *Arabidopsis*. *Planta* **2001**, *212* (4), 598–605.
- (37) Martin, T.; Frommer, W. B.; Salanoubat, M.; Willmitzer, L. Expression of an *Arabidopsis* sucrose synthase gene indicates a role in metabolism of sucrose both during phloem loading and in sink organs. *Plant J.* **1993**, *4* (2), 367–377.
- (38) Dai, N.; Schaffer, A.; Petreikov, M.; Shahak, Y.; Giller, Y.; Ratner, K.; Levine, A.; Granot, D. Overexpression of *Arabidopsis* hexokinase in tomato plants inhibits growth, reduces photosynthesis, and induces rapid senescence. *Plant Cell* **1999**, *11* (7), 1253–1266.
- (39) Gharbi, I.; Ricard, B.; Rolin, D.; Maucourt, M.; Andrieu, M. H.; Bizard, E.; Smiti, S.; Brouquisse, R. Effect of hexokinase activity on tomato root metabolism during prolonged hypoxia. *Plant Cell Environ.* **2007**, *30* (4), 508–517.
- (40) Nairn, C. J.; Lennon, D. M.; Wood-Jones, A.; Nairn, A. V.; Dean, J. F. D. Carbohydrate-related genes and cell wall biosynthesis in vascular tissues of loblolly pine (*Pinus taeda*). *Tree Physiol.* **2008**, *28* (7), 1099–1110.
- (41) Stevenson, G.; Andrianopoulos, K.; Hobbs, M.; Reeves, P. R. Organization of the *Escherichia coli* K-12 gene cluster responsible for production of the extracellular polysaccharide colanic acid. *J. Bacteriol.* **1996**, *178* (16), 4885–4893.
- (42) Gou, J. Y.; Wang, L. J.; Chen, S. P.; Hu, W. L.; Chen, X. Y. Gene expression and metabolite profiles of cotton fiber during cell elongation and secondary cell wall synthesis. *Cell Res.* **2007**, *17* (5), 422–434.
- (43) Li, P. H.; Sioson, A.; Mane, S. P.; Ulanov, A.; Grothaus, G.; Heath, L. S.; Murali, T. M.; Bohnert, H. J.; Grene, R. Response diversity of *Arabidopsis thaliana* ecotypes in elevated [CO₂] in the field. *Plant Mol. Biol.* **2006**, *62* (4), 593–609.
- (44) Radchuk, V.; Sreenivasulu, N.; Radchuk, R.; Wobus, U.; Weschke, W. The methylation cycle and its possible functions in barley endosperm development. *Plant Mol. Biol.* **2005**, *59* (2), 289–307.
- (45) Hoch, J. A.; Nester, E. W. Gene-enzyme relationships of aromatic acid biosynthesis in *Bacillus subtilis*. *J. Bacteriol.* **1973**, *116* (1), 59–66.
- (46) Lewis, N. G.; Davin, L. B.; Sarkany, S. *Lignin and lignan biosynthesis: distinctions and reconciliations*; ACS Publications: Washington, D.C., 1998; p 697.
- (47) Herrmann, K. M. The shikimate pathway: early steps in the biosynthesis of aromatic compounds. *Plant Cell* **1995**, *7* (7), 907–919.
- (48) Sato, K.; Nishikubo, N.; Mashino, Y.; Yoshitomi, K.; Zhou, J. M.; Kajita, S.; Katayama, Y. Immunohistochemical localization of enzymes that catalyze the long sequential pathways of lignin biosynthesis during differentiation of secondary xylem tissues of hybrid aspen (*Populus sieboldii* × *Populus grandidentata*). *Tree Physiol.* **2009**, *29* (12), 1599–1606.
- (49) Richards, T. A.; Dacks, J. B.; Campbell, S. A.; Blanchard, J. L.; Foster, P. G.; McLeod, R.; Roberts, C. W. Evolutionary origins of the eukaryotic shikimate pathway: gene fusions, horizontal gene transfer, and endosymbiotic replacements. *Eukaryot. Cell* **2006**, *5* (9), 1517–1531.
- (50) Goepfert, S.; Poirier, Y. β-Oxidation in fatty acid degradation and beyond. *Curr. Opin. Plant Biol.* **2007**, *10* (3), 245–251.
- (51) Subbaiah, C. C.; Sachs, M. M. Molecular and cellular adaptations of maize to flooding stress. *Ann. Bot.-london* **2003**, *91* (2), 119–127.
- (52) Stevens, M. A. Citrate and malate concentrations in tomato fruits: Genetic control and maturational effects. *J. Am. Soc. Hortic. Sci.* **1972**, *97*, 655–658.
- (53) Rocco, M.; D'Ambrosio, C.; Arena, S.; Faurobert, M.; Scaloni, A.; Marra, M. Proteomic analysis of tomato fruits from two ecotypes during ripening. *Proteomics* **2006**, *6* (13), 3781–3791.
- (54) Page, D.; Gouble, B.; Valot, B.; Bouchet, J.; Callot, C.; Kretzschmar, A.; Causse, M.; Renard, C.; Faurobert, M. Protective proteins are differentially expressed in tomato genotypes differing for their tolerance to low-temperature storage. *Planta* **2010**, *232* (2), 483–500.
- (55) Zhou, D. X.; Hu, Y. F. Regulatory function of histone modifications in controlling rice gene expression and plant growth. *Rice* **2010**, *3* (2–3), 103–111.
- (56) Millar, C. B.; Grunstein, M. Genome-wide patterns of histone modifications in yeast. *Nat. Rev. Mol. Cell Biol.* **2006**, *7* (9), 657–666.
- (57) Costa, R. M. A.; Chigancas, V.; da Silva Galhardo, R.; Carvalho, H.; Menck, C. F. M. The eukaryotic nucleotide excision repair pathway. *Biochimie* **2003**, *85* (11), 1083–1099.
- (58) Kim, Y. O.; Pan, S. O.; Jung, C. H.; Kang, H. A zinc finger-containing glycine-rich RNA-binding protein, atRZ-1a, has a negative impact on seed germination and seedling growth of *Arabidopsis thaliana* under salt or drought stress conditions. *Plant Cell Physiol.* **2007**, *48* (8), 1170–1181.
- (59) Mangeon, A.; Magioli, C.; Menezes-Salgueiro, A. D.; Cardeal, V.; de Oliveira, C.; Galvão, V. C.; Margis, R.; Engler, G.; Sachetto-Martins, G. AtGRPS, a vacuole-located glycine-rich protein involved in cell elongation. *Planta* **2009**, *230* (2), 253–265.
- (60) Liu, L.; Zhou, Y.; Zhou, G.; Ye, R. J.; Zhao, L. N.; Li, X. H.; Lin, Y. J. Identification of early senescence-associated genes in rice flag leaves. *Plant Mol. Biol.* **2008**, *67* (1), 37–55.
- (61) Gubler, F.; Raventos, D.; Keys, M.; Watts, R.; Mundy, J.; Jacobsen, J. V. Target genes and regulatory domains of the GAMYB transcriptional activator in cereal aleurone. *Plant J.* **1999**, *17* (1), 1–9.
- (62) Woodger, F. J.; Millar, A.; Murray, F.; Jacobsen, J. V.; Gubler, F. The role of GAMYB transcription factors in GA-regulated gene expression. *J. Plant Growth Regul.* **2003**, *22* (2), 176–184.
- (63) Kaneko, M.; Inukai, Y.; Ueguchi-Tanaka, M.; Itoh, H.; Izawa, T.; Kobayashi, Y.; Hattori, T.; Miyao, A.; Hirochika, H.; Ashikari, M.; Matsuoka, M. Loss-of-function mutations of the rice GAMYB gene impair α-amylase expression in aleurone and flower development. *Plant Cell* **2004**, *16* (1), 33–44.
- (64) Brockstedt, E.; Otto, A.; Rickers, A.; Bommert, K.; Wittmann-Liebold, B. Preparative high-resolution two-dimensional electrophoresis enables the identification of RNA polymerase B transcription factor 3 as an apoptosis-associated protein in the human BL60–2 Burkitt lymphoma cell line. *J. Protein Chem.* **1999**, *18* (2), 225–231.
- (65) Yang, K. S.; Kim, H. S.; Jin, U. H.; Lee, S. S.; Park, J. A.; Lim, Y. P.; Pai, H. S. Silencing of NbBTF3 results in developmental defects and disturbed gene expression in chloroplasts and mitochondria of higher plants. *Planta* **2007**, *225* (6), 1459–1469.
- (66) Thompson, J. E.; Hopkins, M. T.; Taylor, C.; Wang, T.-W. Regulation of senescence by eukaryotic translation initiation factor 5A: implications for plant growth and development. *Trends Plant Sci.* **2004**, *9* (4), 174–179.
- (67) Feng, H. Z.; Chen, Q. G.; Feng, J.; Zhang, J.; Yang, X. H.; Zuo, J. R. Functional characterization of the *Arabidopsis* eukaryotic

- translation initiation factor 5A-2 that plays a crucial role in plant growth and development by regulating cell division, cell growth, and cell death. *Plant Physiol.* **2007**, *144* (3), 1531–1545.
- (68) Zanelli, C. F.; Maragno, A. L. C.; Gregio, A. P. B.; Komili, S.; Pandolfi, J. R.; Mestriner, C. A.; Lustri, W. R.; Valentini, S. R. eIF5A binds to translational machinery components and affects translation in yeast. *Biochem. Biophys. Res. Commun.* **2006**, *348* (4), 1358–1366.
- (69) Macara, I. G. Transport into and out of the nucleus. *Microbiol. Mol. Biol. Rev.* **2001**, *65* (4), 570–594.
- (70) Weis, K. Nucleocytoplasmic transport: cargo trafficking across the border. *Curr. Opin. Cell Biol.* **2002**, *14* (3), 328–335.
- (71) Rospert, S.; Dubaquie, Y.; Gautschi, M. Nascent-polypeptide-associated complex. *Cell. Mol. Life Sci.* **2002**, *59* (10), 1632–1639.
- (72) Wiedmann, B.; Sakai, H.; Davis, T. A.; Wiedmann, M. A protein complex required for signal-sequence-specific sorting and translocation. *Nature* **1994**, *370*, 434–440.
- (73) Chitteti, B. R.; Peng, Z. H. Proteome and phosphoproteome dynamic change during cell dedifferentiation in *Arabidopsis*. *Proteomics* **2007**, *7* (9), 1473–1500.
- (74) Yan, S. P.; Tang, Z. C.; Su, W. A.; Sun, W. N. Proteomic analysis of salt stress-responsive proteins in rice root. *Proteomics* **2005**, *5* (1), 235–244.
- (75) Hajheidari, M.; Abdollahian-Noghabi, M.; Askari, H.; Heidari, M.; Sadeghian, S. Y.; Ober, E. S.; Hosseini Salekdeh, G. Proteome analysis of sugar beet leaves under drought stress. *Proteomics* **2005**, *5* (4), 950–960.
- (76) Ohyanagi, H.; Tanaka, T.; Sakai, H.; Shigemoto, Y.; Yamaguchi, K.; Habara, T.; Fujii, Y.; Antonio, B. A.; Nagamura, Y.; Imanishi, T.; Ikeo, K.; Itoh, T.; Gojobori, T.; Sasaki, T. The Rice Annotation Project Database (RAP-DB): hub for *Oryza sativa* ssp. *japonica* genome information. *Nucleic Acids Res.* **2006**, *34* (suppl 1), 741–744.
- (77) Amemiya, T.; Kanayama, Y.; Yamaki, S.; Yamada, K.; Shiratake, K. Fruit-specific V-ATPase suppression in antisense-transgenic tomato reduces fruit growth and seed formation. *Planta* **2006**, *223* (6), 1272–1280.
- (78) Young, L.-S.; Harrison, B. R.; Murthy, U. M. N.; Moffatt, B. A.; Gilroy, S.; Masson, P. H. Adenosine Kinase Modulates Root Gravitropism and Cap Morphogenesis in *Arabidopsis*. *Plant Physiol.* **2006**, *142* (2), 564–573.
- (79) Mason, H. S.; Guerrero, F. D.; Boyer, J. S.; Mullet, J. E. Proteins homologous to leaf glycoproteins are abundant in stems of dark-grown soybean seedlings. Analysis of proteins and cDNAs. *Plant Mol. Biol.* **1988**, *11* (6), 845–856.
- (80) Cai, G. Assembly and disassembly of plant microtubules: tubulin modifications and binding to MAPs. *J. Exp. Bot.* **2010**, *61* (3), 623–626.
- (81) Hussey, P. J.; Ketelaar, T.; Deeks, M. J. Control of the actin cytoskeleton in plant cell growth. *Annu. Rev. Plant Biol.* **2006**, *57* (1), 109–125.
- (82) Mustroph, A.; Lee, S. C.; Oosumi, T.; Zanetti, M. E.; Yang, H. J.; Ma, K.; Yaghoubi-Masihi, A.; Fukao, T.; Bailey-Serres, J. Cross-Kingdom comparison of transcriptomic adjustments to low-oxygen stress highlights conserved and plant-specific responses. *Plant Physiol.* **2010**, *152* (3), 1484–1500.
- (83) Fukao, T.; Xu, K.; Ronald, P. C.; Bailey-Serres, J. A variable cluster of ethylene response factor-like genes regulates metabolic and developmental acclimation responses to submergence in rice. *Plant Cell* **2006**, *18* (8), 2021–2034.
- (84) Mittler, R.; Vanderauwera, S.; Gollery, M.; Van Breusegem, F. Reactive oxygen gene network of plants. *Trends Plant Sci.* **2004**, *9* (10), 490–498.
- (85) Cosgrove, D. J. Loosening of plant cell walls by expansins. *Nature* **2000**, *407* (6802), 321–326.
- (86) Kwon, S. I.; Lee, H.; An, C. S. Differential expression of three catalase genes in the small radish (*Raphanus sativus* L. var. *sativus*). *Mol. Cells* **2007**, *24* (1), 37–44.
- (87) Foreman, J.; Demidchik, V.; Bothwell, J. H. F.; Mylona, P.; Miedema, H.; Torres, M. A.; Linstead, P.; Costa, S.; Brownlee, C.; Jones, J. D. G. Reactive oxygen species produced by NADPH oxidase regulate plant cell growth. *Nature* **2003**, *422* (6930), 442–446.
- (88) Sauter, M.; Rzewuski, G.; Marwedel, T.; Lorbiecke, R. The novel ethylene-regulated gene *OsUsp1* from rice encodes a member of a plant protein family related to prokaryotic universal stress proteins. *J. Exp. Bot.* **2002**, *53* (379), 2325–2331.